Timing jitter of femtosecond solitons in single-mode optical fibers: A perturbation model

Shihua Chen,* Dufang Shi, and Lin Yi

*Department of Physics and State Key Laboratory of Laser Technology, Huazhong University of Science and Technology,
Wuhan 430074, People's Republic of China*

On the basis of the higher-order nonlinear Schrödinger equation, an extended soliton perturbation model is proposed. The evolution equations for the soliton parameters and the resultant expressions for timing jitter are derived. Subsequently, the model is tested to be correct in the subpicosecond-femtosecond regime through direct numerical simulations of the underlying equation by using the stochastic split-step Fourier method. It is shown that the results of our numerical simulations are in excellent agreement with analytical predictions for timing jitter. It is found that the Gordon-Haus jitter for dark solitons is nearly $1/\sqrt{2}$ of that for bright solitons, and that the Raman jitter always dominates the Gordon-Haus jitter in the femtosecond regime. In particular, the stabilities of the solitary waves are demonstrated under the Gaussian white noise. It is expected that for bright and dark solitons, the present equations of motion would find extensive applications in the high-speed communication systems more than those obtained by use of the well-known perturbation theory about the nonlinear Schrödinger equation [J. Opt. Soc. Am. B **18**, 153 (2001)].

I. INTRODUCTION

The soliton concept is a sophisticated mathematical construct based on the complete integrability of a class of nonlinear partial differential equations which can pass the Painlevé test and can be solved via the inverse scattering transform [1]. Physically, there are two different mechanisms which make an optical pulse propagation a soliton or solitary wave. One, given by Hasegawa and Tappert, is the balance between the pulse broadening of the group-velocity dispersion (GVD) and the compressing of the Kerr nonlinearity, which is governed by the well-analyzed nonlinear Schrödinger (NLS) equation [2]. The other, proposed by McCall and Hahn, is due to the self-induced transparency in a resonant medium and is described by the Maxwell-Bloch equations [3]. In this paper, we are concerned with femtosecond soliton propagation in single-mode optical fibers, which belongs to the former case.

Over short distances and in weak nonlinear medium, the NLS equation can lead to a soliton behavior applicable to a picosecond regime, whereas over longer distances or for an initial high intense ultrashort pulse a number of higher-order effects such as the third-order dispersion (TOD), self-steepening [4], and the self-frequency shift (SFS) [5] must be taken into account. Thus, the classical NLS equation fails in the physical description of soliton behavior under the circumstances. In recent literature, some authors pointed out that the higher-order nonlinear Schrödinger (HONLS) equation derived by Kodama and Hasegawa [6] can be used to describe the soliton behavior in a subpicosecond-femtosecond regime [7–11]. Moreover, both bright- and dark-soliton solutions were given there under certain parametric conditions.

In the current decade, physicists [12–15] have elucidated with sufficient accuracy some phenomenological effects, e.g., soliton noise or timing jitter, by means of the perturbation theory about the NLS equation developed by Haus and Lai [12]. In particular, Drummond *et al.* [13] showed that intrinsic thermal quantum noise from phonon reservoirs, which depends strongly on both the temperature and pulse intensity, contributes more largely to timing jitter than does the gain-related Gordon-Haus noise [14] for femtosecond solitons. For simplicity, they ignored the self-frequency shift and Kerr dispersion. Following the procedures developed by Drummond *et al.* [13] and Haus *et al.* [12,15] we propose an extended soliton perturbation model, based on the HONLS equation. As a result, the evolution equations of soliton parameters and the analytical expressions for timing jitter are respectively derived for bright and dark solitons. Therein we have considered TOD and Kerr dispersion. By checking the analytical predictions for timing jitter against direct numerical simulations, we show that the results obtained by this model are correct in the subpicosecond-femtosecond regime and are more generic than those obtained before [13,15], since those higher-order effects are included.

The paper is organized as follows. The generalized NLS equation for femtosecond solitons propagating in single-mode, polarization-preserving optical fibers will be cited in Sec. II, where the corresponding bright- and dark-soliton solutions for the HONLS equation are given. More significantly, the stabilities of the solitonlike solutions under Gaussian white noise are also demonstrated numerically. In Sec. III, we propose an extended soliton perturbation model based on the HONLS equation and derive the resultant evolution equations for the soliton parameters and the corresponding expressions for timing jitter for bright and dark solitons. In order to check our theoretical model, an efficient simulating scheme in terms of the stochastic split-step Fourier method is outlined in Sec. IV. Comparing our analytical calculations with numerical simulations, various timing jitters are discussed in Sec. V. Finally, our results are concluded in Sec. VI.

II. GENERALIZED NLS EQUATION

The generalized nonlinear propagation equation governing the evolution of femtosecond optical field ψ in single-

---

*Electronic address: cshua@mail.edu.cn

mode optical fibers was derived by Kodama and Hasegawa [6]. In the context of soliton propagation, it is useful to employ a renormalization in the propagative reference frame of $\tau = (t - z/v)/T_0$ and $\zeta = z/L_D$, where T_0 is a typical initial soliton duration, and $L_D = T_0^2/|\beta_2|$ denotes the dispersion length at carrier frequency ω_0. By including the noise sources [13], the generalized NLS equation can be rewritten as

$$\psi_\zeta = \pm \frac{i}{2}\psi_{\tau\tau} + i|\psi|^2\psi + \frac{1}{6}\alpha_1\psi_{\tau\tau\tau} - \gamma\psi - \alpha_2(|\psi|^2\psi)_\tau$$
$$- \alpha_3\psi(|\psi|^2)_\tau + i\Gamma^R\psi + \Gamma, \qquad (1)$$

where a shorthand $\psi = \psi(\zeta, \tau)$ is exploited for brevity; thus is a dimensionless photon field, and the subscripts ζ and τ denote the spatial and temporal partial derivatives. The term related to γ accounts for the fiber net loss through the relation $\gamma = (\gamma^A - \gamma^G)L_D/v$, where γ^A and γ^G denote the corresponding absorption and gain coefficients. The parameters $\beta_m \equiv [d^m\beta/d\omega^m]_{\omega=\omega_0}$ with, $m = 1,2,3$, result from an expansion of the propagation constant $\beta(\omega)$ in a Taylor series. Physically, the group velocity v is simply the inverse of the parameter β_1. The parameter α_1 is responsible for the TOD and is defined as $\alpha_1 = \beta_3/T_0|\beta_2|$, while the terms related to α_2 and α_3 describe the effects of self-steepening and the SFS arising from stimulated Raman scattering, respectively. Although self-steepening and the SFS are negligible in a picosecond regime, they are of considerable importance when the pulses are shorter than 100 fs. The positive sign in front of the second derivative term applies for an anomalous dispersion ($\beta_2 < 0$), which occurs for longer wavelengths, whereas the negative sign applies for normal dispersion ($\beta_2 > 0$). The model parameters α_1 and γ are real constants; α_2 and α_3 can be complex [6,16]. Here for simplicity, we have assumed that the coefficients α_2 and α_3 are also real constants and the inequality $3\alpha_2 + 2\alpha_3 > 0$ is always met.

It should be noted that in Eq. (1), the Raman noise and gain-related Gordon-Haus noise appear, respectively, as the real multiplicative stochastic variable Γ^R and the complex additive stochastic variable Γ, which are responsible for the timing jitter occurring in the soliton communication systems [13,17–21]. According to the generalized Wiener-Khintchine theorem [22], the spatiotemporal correlations of stochastic variables can be expressed as [13]

$$\langle\Gamma^R(\zeta,\tau)\Gamma^R(\zeta',\tau')\rangle = \frac{1}{\bar{n}}F(\tau-\tau')\delta(\zeta-\zeta'),$$

$$\langle\Gamma^*(\zeta,\tau)\Gamma(\zeta',\tau')\rangle = \frac{\alpha^G}{\bar{n}}\delta(\tau-\tau')\delta(\zeta-\zeta'), \qquad (2)$$

$$\langle\Gamma(\zeta,\tau)\Gamma^*(\zeta',\tau')\rangle = \frac{\alpha^A}{\bar{n}}\delta(\tau-\tau')\delta(\zeta-\zeta'),$$

where $\alpha^G = 2\gamma^G L_D/v$, $\alpha^A = 2\gamma^A L_D/v$, $\bar{n} = v^2 T_0/\chi L_D$ is the typical number of photons in a soliton pulse, χ

$= hn_2\omega_0^2 v^2/(2\pi A_{\text{eff}}c)$ is the effective nonlinear susceptibility resulting from the electronic Kerr and Raman contributions, A_{eff} is known as the effective mode area, n_2 is the nonlinear refractive index, and c and $h = 2\pi\hbar$ represent the speed of light and the Planck constant, respectively. The time correlation function is given by

$$F(\tau) = \frac{1}{2\pi}\int \exp(-i\omega\tau)\alpha^R(\omega)\left[n_{\text{th}}(|\omega|/T_0) + \frac{1}{2}\right]d\omega, \qquad (3)$$

where $\alpha^R(\omega)$ is the Raman gain coefficient [13,23], and $n_{\text{th}}(\omega) = [\exp(\hbar\omega/k_B T) - 1]^{-1}$ denotes the thermal Bose-Einstein distribution, with k_B the Boltzmann's constant and T the temperature. It is easy to show that if the gain and loss in the fiber are broadband relative to the soliton bandwidth and balance exactly, i.e., $\gamma = 0$, and the noise sources are negligible, Eq. (1) can be reduced to the familiar HONLS equation:

$$\psi_\zeta = \frac{i}{2}\alpha_0\psi_{\tau\tau} + i|\psi|^2\psi + \frac{1}{6}\alpha_1\psi_{\tau\tau\tau} - \alpha_2(|\psi|^2\psi)_\tau$$
$$- \alpha_3\psi(|\psi|^2)_\tau, \qquad (4)$$

where $\alpha_0 = \text{sgn}(-\beta_2)$. The five terms on the right-hand side of Eq. (4) account for the GVD, self-phase modulation (SPM), TOD, self-steepening, and the SFS arising from stimulated Raman scattering, respectively. When the last three terms are omitted, Eq. (4) reduces to the well-known NLS equation. As compared with the GVD and SPM which produce symmetric broadening in the time and frequency domain, respectively, and counterbalance to propagate solitons under certain parametric conditions, these higher-order effects cause asymmetrical broadening either temporally or spectrally and also have the possibilities to yield soliton propagation [10]. After an appropriate transformation, the bright-soliton solution of Eq. (4), where $\alpha_0 = 1$, reads [7,8,11]

$$\psi_0(\zeta,\tau) = mA\,\text{sech}[A\tau + q(\zeta)]\exp[-i\Omega\tau + i\theta(\zeta)], \quad (5)$$

where

$$m = \left(\frac{-\alpha_1}{3\alpha_2 + 2\alpha_3}\right)^{1/2}, \quad (\alpha_1 < 0),$$

$$\Omega = \frac{3\alpha_2 + 2\alpha_3 + \alpha_1}{2\alpha_1(\alpha_2 + \alpha_3)},$$

$$\frac{dq(\zeta)}{d\zeta} = \frac{1}{6}\alpha_1 A^3 - \frac{1}{2}\alpha_1 A\Omega^2 + A\Omega, \qquad (6)$$

$$\frac{d\theta(\zeta)}{d\zeta} = \frac{1}{2}(1 - \alpha_1\Omega)A^2 + \frac{1}{6}\alpha_1\Omega^3 - \frac{1}{2}\Omega^2.$$

When $\alpha_0 = -1$, the dark-soliton solution of Eq. (4) can be written as [9,11]

$$\psi_0(\zeta,\tau) = nB\tanh[B\tau - Q(\zeta)]\exp[-i\varpi\tau + i\vartheta(\zeta)], \quad (7)$$

where

$$n = \left(\frac{\alpha_1}{3\alpha_2 + 2\alpha_3} \right)^{1/2}, \quad (\alpha_1 > 0),$$

$$\varpi = \frac{\alpha_1 - 3\alpha_2 - 2\alpha_3}{2\alpha_1(\alpha_2 + \alpha_3)},$$

$$\frac{dQ(\zeta)}{d\zeta} = \frac{1}{3}\alpha_1 B^3 + \frac{1}{2}\alpha_1 B \varpi^2 + B\varpi, \quad (8)$$

$$\frac{d\vartheta(\zeta)}{d\zeta} = (1 + \alpha_1 \varpi)B^2 + \frac{1}{6}\alpha_1 \varpi^3 + \frac{1}{2}\varpi^2.$$

Obviously, either solution (5) or (7) has only one independent intrinsic parameter A or B since the parameter Ω or ϖ is fixed [7,17]. It is noted that there exists a proper subset of conditions, to name a few, $\alpha_1 : \alpha_2 : \alpha_3 = \mp 6:6:-6$ (Hirota), or $\mp 6:6:-3$ (Sasa-Satsuma), under which Eq. (4) is completely integrable [7]. In the cases beyond these conditions, solutions (5) and (7) are not true solitons in a strict mathematical sense, but share some properties with solitons such as preserving shape and size during propagation [24]. It is of interest to note that these solutions are not compatible with the respective counterparts of the standard NLS equation [11]. But, as in an integrable case, these solitons or solitary waves in our Hamiltonian systems (but nonintegrable) can also be regarded as nonlinear modes, and allow us to describe the behavior of systems with an infinite number of degrees of freedom in terms of a few variables (see, e.g., Ref. [25]). For brevity, our localized waves under consideration are loosely called ''solitons'' even though this is a terminology reserved for integrable sets.

Because all physical systems are dispersive and dissipative in reality, an investigation of the stabilities of these solitons is of great significance [16]. In order to test the stabilities of solitons, the underlying equation (1) is directly simulated by using the stochastic split-step Fourier method (see Sec. IV). Figures 1 and 2 show the evolutions of these $T_0 = 500$ fs bright and dark solitons under perturbations of Gaussian white noise, respectively. It is striking that the solitons of motion are stable. Here the dimensionless model parameters are $\alpha_1 = \mp 9.6 \times 10^{-3}$, $\alpha_2 = 3.18 \times 10^{-3}$, and $\alpha_3 = (\mp \alpha_1 - 3\alpha_2)/2$. These parameters can be determined by several basic fiber parameters such as $\beta_2 = \mp 0.5$ ps^2/km and $\beta_3 = \mp 0.0024$ ps^3/km, where negative and positive signs correspond to the bright and dark solitons, respectively. Compared with Fig. 1, Fig. 3 displays the evolution of a bright soliton with the same initial duration T_0 but with different model parameters, where $\alpha_1 = -0.056$, $\alpha_2 = 3.18 \times 10^{-3}$, and $\alpha_3 = -(\alpha_1 + 3\alpha_2)/2$. These values are subject to another set of fiber parameters $\beta_2 = -2.5$ ps^2/km, and $\beta_3 = -0.07$ ps^3/km. It is clear that these solitons, apart from undergoing a temporal shift, are rather stable against some finite perturbations in a broad parameter range. Their profiles or shapes are well preserved after propagating a long distance of a few thousands of dispersion lengths as shown in those insets of Figs. 1, 2, and 3, which
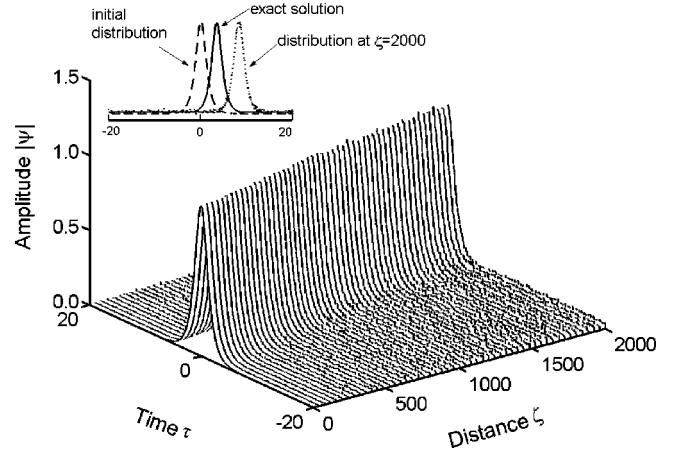

FIG. 1. Evolution of the 500-fs bright soliton under the perturbation of Gaussian white noise. In our simulation of Eq. (1), two dimensionless steps $\Delta\zeta = 0.04$ and $\Delta\tau = 0.005$ are used in the discretization and $\psi^{\text{bri}}(0,\tau)$ is chosen as initial pulse, where $\alpha_1 = -9.6 \times 10^{-3}$, $\alpha_2 = 3.18 \times 10^{-3}$, and $\alpha_3 = -(\alpha_1 + 3\alpha_2)/2$. The inset shows a comparison of pulses at $\zeta = 0$ and 2000 as well as an exact distribution without noise.

show comparisons of pulses at typical distances ζ with the initial distributions as well as exact solutions without noise.

As usual, Eq. (1) can be solved in terms of the moment method [19], or the perturbation theory that treats all high-order effects and noise sources as a small perturbation to the well-analyzed NLS equation [26]. Corresponding to our proposed system, however, we find that there exists a relatively simpler alternative in which one can take only the stochastic terms as a small perturbation to the HONLS equation. Detailed treatments of the problem will be provided in Sec. III.

III. SOLITON PERTURBATION MODEL

Before proceeding, we would like to discuss the adiabatic perturbation theory (APT) about femtosecond solitons,
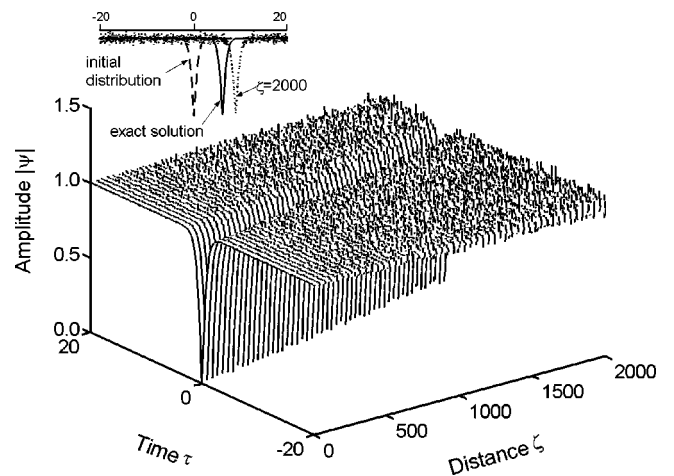

FIG. 2. Evolution of the 500-fs dark soliton under the perturbation of Gaussian white noise. The discretized steps are the same as Fig. 1, but $\psi^{\text{dar}}(0,\tau)$ is chosen as the initial pulse. Here the parameters are $\alpha_1 = 9.6 \times 10^{-3}$, $\alpha_2 = 3.18 \times 10^{-3}$, and $\alpha_3 = (\alpha_1 - 3\alpha_2)/2$. The inset shows a comparison of pulses at $\zeta = 0$ and 2000 as well as an exact distribution without noise.
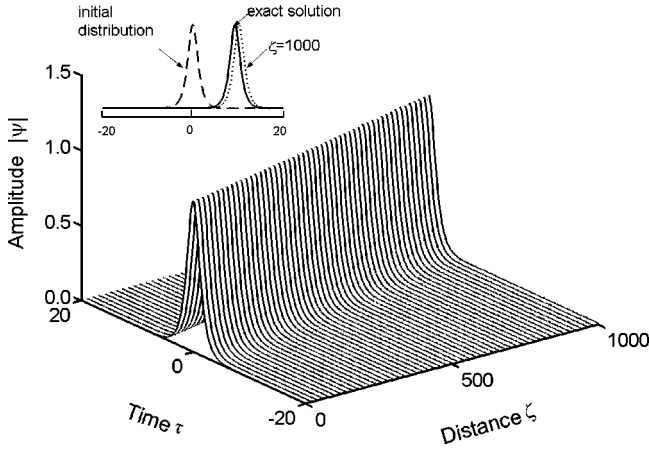
FIG. 3. Evolution of the 500-fs bright soliton under the perturbation of Gaussian white noise, where $\alpha_1 = -0.056$, $\alpha_2 = 3.18 \times 10^{-3}$, and $\alpha_3 = -(\alpha_1 + 3\alpha_2)/2$. The other parameters are the same as in Fig. 1. The inset shows a comparison of pulses at $\zeta = 0$, and 1000 as well as an exact distribution without noise.

which has been used successfully to investigate the timing jitter in the high-speed soliton communication systems [18]. In the following, we wish to propose an extended soliton perturbation model and derive the evolution equations for the soliton parameters. Solving these equations, we shall obtain approximately the analytical formulas of timing jitter for bright and dark solitons.

Now, we apply the APT to Eq. (1) by taking its unperturbed solution as a fundamental soliton of the form of solution (5) [or Eq. (7)], where parameter Ω (or ϖ) is assumed to be a variable just like the parameter A or B, and all parameters A, Ω, q, and θ (or B, ϖ, Q, and ϑ) vary with distance ζ slowly. Furthermore, we treat the noise term $\bar{\Gamma} = i\Gamma^R \psi_0 + \Gamma$ on the right-hand side of Eq. (1) as a small perturbation. The evolution equations for the bright soliton parameters are therefore governed by

$$\frac{dA}{d\zeta} = \mathrm{Re} \int U_A \bar{\Gamma} \, d\tau,$$

$$\frac{d\theta}{d\zeta} = -\frac{1}{6}(1 - \alpha_1 \Omega)A^2 + \frac{1}{6}\alpha_1 \Omega^3 - \frac{1}{2}\Omega^2$$

$$+ \frac{2}{3}m^2(1 + \alpha_2 \Omega)A^2 + \mathrm{Im} \int U_\theta \bar{\Gamma} \, d\tau,$$

$$(9)$$

$$\frac{dq}{d\zeta} = \frac{1}{6}\alpha_1 A^3 - \frac{1}{2}\alpha_1 A\Omega^2 + A\Omega + \mathrm{Re} \int U_q \bar{\Gamma} \, d\tau,$$

$$\frac{d\Omega}{d\zeta} = \mathrm{Im} \int U_\Omega \bar{\Gamma} \, d\tau,$$

where "Re" and "Im" stand for real and imaginary parts of the whole integral, respectively. The projection functions for bright solitons are given by

$$U_A = \frac{1}{m^2} \psi_0^*,$$

$$U_\theta = \frac{1}{m^2 A}\left[\frac{1}{2} + q \tanh(A\tau + q)\right]\psi_0^*,$$

$$U_q = -\frac{1}{m^2}\tau\psi_0^*, \qquad (10)$$

$$U_\Omega = -\frac{1}{m^2}\tanh(A\tau + q)\psi_0^*.$$

In the same way, the equations of motion for the dark soliton parameters are found readily to be

$$\frac{dB}{d\zeta} = \mathrm{Re} \int U_B \bar{\Gamma} \, d\tau,$$

$$\frac{d\vartheta}{d\zeta} = \frac{1}{3}(1 + \alpha_1 \varpi)B^2 + \frac{1}{6}\alpha_1 \varpi^3 + \frac{1}{2}\varpi^2 + \frac{2}{3}n^2(1 + \alpha_2 \varpi)B^2$$

$$+ \mathrm{Im} \int U_\vartheta \bar{\Gamma} \, d\tau,$$

$$(11)$$

$$\frac{dQ}{d\zeta} = \frac{1}{3}\alpha_1 B^3 + \frac{1}{2}\alpha_1 B\varpi^2 + B\varpi + \mathrm{Re} \int U_Q \bar{\Gamma} \, d\tau,$$

$$\frac{d\varpi}{d\zeta} = \mathrm{Im} \int U_\varpi \bar{\Gamma} \, d\tau,$$

where the projection functions take the forms

$$U_B = \frac{1}{n}\frac{B \tanh(B\tau - Q)}{\cosh^2(B\tau - Q)}\exp[i\varpi\tau - i\vartheta],$$

$$U_\vartheta = \frac{1}{n}\frac{B\tau - 2Q}{\cosh^2(B\tau - Q)}\exp[i\varpi\tau - i\vartheta],$$

$$U_Q = \frac{1}{n}\frac{Q \tanh(B\tau - Q) - 3/4}{\cosh^2(B\tau - Q)}\exp[i\varpi\tau - i\vartheta], \quad (12)$$

$$U_\varpi = -\frac{1}{n}B \, \mathrm{sech}^2(B\tau - Q)\exp[i\varpi\tau - i\vartheta].$$

It is straightforward to prove that when the noise sources vanish, Eqs. (9) and (11) reduce to Eqs. (5) and (7), respectively. For heuristical discussion, we illustrate the evolution of a bright soliton in Fig. 4 with the same conditions as in Fig. 1, but with a direct numerical simulation of Eq. (9). In essence, these sets of stochastic differential equations agree well with Eq. (1) within their errors, especially for picosecond solitons [18]. Therefore, our Eqs. (9)–(12) can be applied to the numerical study of timing jitter. On the other hand, two parameters Ω and ϖ in these equations fluctuate with the noise term $\bar{\Gamma}$ and become of stochastic functions of
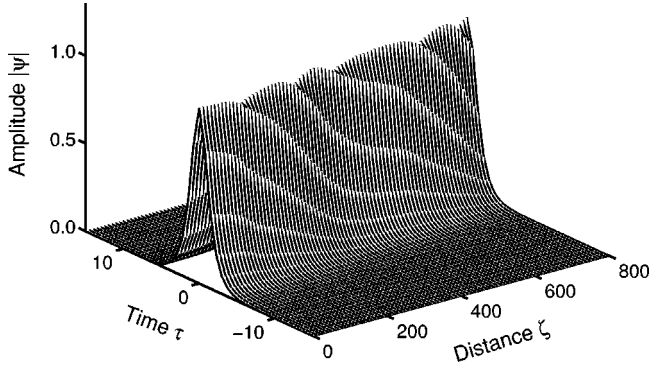
FIG. 4. Evolution of the 500-fs bright soliton under the perturbation of Gaussian white noise, where we simulate Eq. (9) and use $\Delta\zeta=0.01$ and $\Delta\tau=0.015$. The other conditions are the same as in Fig. 1.

distance. Thus, it is reasonable to take Ω as the frequency variable of bright soliton and ϕ related to ϖ as the phase shift of dark soliton [13,21] in the following subsections.

A. Bright solitons

Following the method developed by Haus and Lai [12], we treat the effect of the noise term as a perturbation to the solution of a bright soliton whose parameters vary slowly with

$$\psi(\zeta,\tau)=\psi_0(\zeta,\tau)+\Delta\psi(\zeta,\tau), \tag{13}$$

where $\psi_0(\zeta,\tau)$ is given by the Eq. (5). For simplicity, we shall study the case $\alpha_1+3\alpha_2+2\alpha_3=0$ in this paper. Although the situation $\alpha_1+3\alpha_2+2\alpha_3\neq0$ is a little complicated, one could deal with it in a similar fashion. Furthermore, the bright-soliton solution (5) reduces to

$$\psi_0(\zeta,\tau)=A\,\text{sech}[A\tau+q(\zeta)]\exp[i\theta(\zeta)], \tag{14}$$

where

$$q(\zeta)=\frac{1}{6}\alpha_1 A^3\zeta, \quad \theta(\zeta)=\frac{1}{2}A^2\zeta.$$

Substituting Eq. (13) into Eq. (1) and neglecting higher order terms than $\Delta\psi$, with some manipulations, we have

$$[\Delta\psi]_\zeta=\frac{i}{2}\alpha_0[\Delta\psi]_{\tau\tau}+i[\psi_0^2\Delta\psi^*+2|\psi_0|^2\Delta\psi]$$

$$+\frac{1}{6}\alpha_1[\Delta\psi]_{\tau\tau\tau}-\alpha_2[\psi_0^2\Delta\psi^*+2|\psi_0|^2\Delta\psi]_\tau$$

$$-\alpha_3[|\psi_0|^2]_\tau\Delta\psi-\alpha_3[\psi_0^*\Delta\psi+\psi_0\Delta\psi^*]_\tau\psi_0+\bar{\Gamma}, \tag{15}$$

where $\alpha_0=1$ for bright solitons.

To solve Eq. (15), the perturbed term $\Delta\psi$ can be approximated as a superposition of changes in the four soliton parameters A, θ, q, and Ω, plus a continuum term $\Delta\psi_c$,

$$\Delta\psi=f_A(\zeta,\tau)\Delta A(\zeta)+f_\theta(\zeta,\tau)\Delta\theta(\zeta)+f_q(\zeta,\tau)\Delta q(\zeta)$$

$$+f_\Omega(\zeta,\tau)\Delta\Omega(\zeta)+\Delta\psi_c, \tag{16}$$

where the perturbation functions $f_{X_i}(\zeta,\tau)$ are derivatives of $\psi_0(\zeta,\tau)$ with respect to X_i, where $X_i=A$, θ, q, and Ω. It is noted that $\Delta A(\zeta)$, $\Delta\theta(\zeta)$, $\Delta q(\zeta)$, and $\Delta\Omega(\zeta)$ are real functions of distance ζ. After a little algebra, we find

$$f_A(\zeta,\tau)=\frac{\partial}{\partial A}\psi_0(\zeta,\tau)=[1/A-\tau\tanh(A\tau+q)]\psi_0,$$

$$f_\theta(\zeta,\tau)=\frac{\partial}{\partial\theta}\psi_0(\zeta,\tau)=i\psi_0,$$

$$f_q(\zeta,\tau)=\frac{\partial}{\partial q}\psi_0(\zeta,\tau)=-\tanh(A\tau+q)\psi_0, \tag{17}$$

$$f_\Omega(\zeta,\tau)=\frac{\partial}{\partial\Omega}\psi_0(\zeta,\tau)=-i\tau\psi_0.$$

Because Eq. (15) is not self-adjoint, these functions in Eq. (17) are not orthogonal. In order to project out the evolution of a particular parameter, we therefore choose an alternative set of functions $\overline{f_{X_i}}(\zeta,\tau)$ as

$$\overline{f_A}(\zeta,\tau)=\psi_0,$$

$$\overline{f_\theta}(\zeta,\tau)=i\left(\tau+\frac{2q}{A}\right)\tanh(A\tau+q)\psi_0,$$

$$\overline{f_q}(\zeta,\tau)=-\tau\psi_0, \tag{18}$$

$$\overline{f_\Omega}(\zeta,\tau)=-i\tanh(A\tau+q)\psi_0,$$

which are the eigenfunctions of the adjoint equation to Eq. (15) and are orthonormal to the set in Eq. (17), i.e.,

$$\text{Re}\int_{-\infty}^{\infty}\overline{f_{X_i}}^*(\zeta,\tau)f_{X_j}(\zeta,\tau)d\tau=\delta_{i,j}. \tag{19}$$

Because the group velocity for any linear perturbation is different from the propagation velocity of the soliton, the perturbation acting on soliton will disperse and/or move away from the soliton. Therefore, the continuum $\Delta\psi_c$ is also orthogonal to $\overline{f_{X_i}}(\zeta,\tau)$ under the circumstances [12,13,15].

By substituting Eq. (16) into Eq. (15) and using the orthogonal relation (19), the four equations of motion for the soliton parameters can be derived as (see the Appendix)

$$[\Delta A]_\zeta=\Gamma_A(\zeta),$$

$$[\Delta\theta]_\zeta=A\Delta A+\frac{1}{6}(2\alpha_2-\alpha_1)A^2\Delta\Omega+\Gamma_\theta(\zeta),$$

$$[\Delta q]_\zeta=A\Delta\Omega+\frac{1}{2}\alpha_1 A^2\Delta A+\Gamma_q(\zeta), \tag{20}$$

$$[\Delta\Omega]_\zeta = \Gamma_\Omega(\zeta),$$

where the noise sources are given by

$$\Gamma_{X_i}(\zeta) = \mathrm{Re} \int_{-\infty}^{\infty} \overline{f_{X_i}}^*(\zeta,\tau)\bar{\Gamma}\, d\tau. \tag{21}$$

It should be emphasized that the third formula in Eq. (20) describes the dependence of position fluctuations $\Delta q(\zeta)$ on both frequency fluctuations $\Delta\Omega(\zeta)$ and amplitude fluctuations $\Delta A(\zeta)$ when the parameter α_1 is non-negligible. This effect is of great importance for femtosecond solitons. Provided that the TOD, self-steepening, and SFS effects are not considered, Eq. (20) reduces to the case of picosecond solitons [see, e.g., Eqs. (4.7)–(4.10) in Ref. [15]].

If choosing a multimode coherent state as the initial condition, that is, for coherent inputs, the Wigner vacuum fluctuations are Gaussian and are correlated as

$$\langle \Delta\psi^*(0,\tau)\Delta\psi(0,\tau')\rangle = \frac{1}{2\bar{n}}\delta(\tau-\tau'); \tag{22}$$

then, upon integrating the first and fourth formulas in Eq. (20), two correlations related to the fluctuations in amplitude and frequency can be given by

$$\langle \Delta A^*(\zeta)\Delta A(\zeta')\rangle = \langle \Delta A^*(0)\Delta A(0)\rangle$$
$$+ \int_0^\zeta \int_0^{\zeta'} \langle \Gamma_A^*(\zeta'')\Gamma_A(\zeta''')\rangle d\zeta'' d\zeta'''$$
$$= \frac{A}{2\bar{n}} + \frac{A\alpha^G}{\bar{n}}\zeta, \quad \zeta < \zeta', \tag{23}$$

$$\langle \Delta\Omega^*(\zeta)\Delta\Omega(\zeta')\rangle = \langle \Delta\Omega^*(0)\Delta\Omega(0)\rangle$$
$$+ \int_0^\zeta \int_0^{\zeta'} \langle \Gamma_\Omega^*(\zeta'')\Gamma_\Omega(\zeta''')\rangle d\zeta'' d\zeta'''$$
$$= \frac{A}{6\bar{n}} + \frac{A}{3\bar{n}}[\alpha^G + 6A\mathcal{I}(A)]\zeta, \quad \zeta < \zeta', \tag{24}$$

where $\Delta X_i(0) = \mathrm{Re}\int \overline{f_{X_i}}^*(0,\tau)\Delta\psi(0,\tau)d\tau$, and the overlap integral $\mathcal{I}(X)$ is defined as

$$\mathcal{I}(X) = \int_{-\infty}^{\infty}\int_{-\infty}^{\infty} \frac{\tanh\tau\tanh\tau'}{2\cosh^2\tau\cosh^2\tau'}F\left(\frac{\tau-\tau'}{X}\right)d\tau\, d\tau'. \tag{25}$$

In the derivations of Eqs. (23) and (24), we have used the stochastic correlations in Eq. (2), and the fundamental knowledge such as $\langle \mathrm{Re}\,\Gamma^*(\zeta,\tau)\mathrm{Re}\,\Gamma(\zeta',\tau')\rangle = (1/2)\mathrm{Re}\langle\Gamma^*(\zeta,\tau)\Gamma(\zeta',\tau')\rangle$ [22].

The correlation in position fluctuations corresponds to the timing jitter in arrival times since we have chosen a propagative reference frame. Therefore the jitter feeds off position fluctuations as well as off noises entering through the frequency and amplitude. By using Eqs. (20), (23), and (24), the jitter variance can be written as

$$\sigma_q^2 = \langle \Delta q^*(\zeta)\Delta q(\zeta)\rangle$$
$$= \langle \Delta q^*(0)\Delta q(0)\rangle$$
$$+ A^2 \int_0^\zeta \int_0^\zeta \langle \Delta\Omega^*(\zeta'')\Delta\Omega(\zeta''')\rangle d\zeta'' d\zeta'''$$
$$+ \frac{1}{4}\alpha_1^2 A^4 \int_0^\zeta \int_0^\zeta \langle \Delta A^*(\zeta'')\Delta A(\zeta''')\rangle d\zeta'' d\zeta'''$$
$$+ \alpha_1 A^2 \int_0^\zeta \int_0^\zeta \langle \Delta A^*(\zeta'')\Gamma_q(\zeta''')\rangle d\zeta'' d\zeta'''$$
$$+ \int_0^\zeta \int_0^\zeta \langle \Gamma_q^*(\zeta'')\Gamma_q(\zeta''')\rangle d\zeta'' d\zeta'''$$
$$= \sigma_I^2 + \sigma_{GH}^2 + \sigma_R^2. \tag{26}$$

It should be pointed out that other correlations undisplayed above are equal to zero. Here σ_I^2, σ_{GH}^2, and σ_R^2 correspond to the mean-square timing jitter resulting from the vacuum fluctuations, the Gordon-Haus effect, and Raman noise, respectively. We find

$$\sigma_I^2 = \frac{\pi^2}{24\bar{n}A} + \left[\frac{1}{6\bar{n}} + \frac{\alpha_1^2 A^2}{8\bar{n}}\right]A^3\zeta^2,$$

$$\sigma_{GH}^2 = \frac{\pi^2\alpha^G}{12\bar{n}A}\zeta + \left[\frac{1}{9\bar{n}} + \frac{13\alpha_1^2 A^2}{108\bar{n}}\right]\alpha^G A^3\zeta^3, \tag{27}$$

$$\sigma_R^2 = \frac{2\mathcal{I}(A)}{3\bar{n}}A^4\zeta^3.$$

The resulting formulas (27) are not only useful in the femtosecond regime, but are also applicable to the picosecond regime. In the picosecond regime, α_1 is much less than 1. Thus all terms associated with α_1 in Eq. (27) can be neglected. But the mean-square Gordon-Haus jitter, σ_{GH}^2, still has a cubic growth with distance. Our result coincides with the conclusion reported by Haus and co-workers [14,15]. In the femtosecond regime, these mean-square jitters, except the Raman one which seems to be immune to the higher-order effects, have an extra quadratic or cubic growth and depend strongly on the magnitude of α_1. Indeed, if $\Omega \neq 0$ is considered, the mean-square Raman jitter also depends on the higher-order effects, where $\sigma_R^2 = 2(1-\alpha_1\Omega)^2\mathcal{I}(A)A^4\zeta^3/3\bar{n}$.

B. Dark solitons

In the normal dispersion regime ($\alpha_1 > 0$), the HONLS equation has a dark-soliton solution described by Eq. (7). In analogy to bright solitons, we consider the most simple case $\varpi = 0$, i.e., the relation $\alpha_1 = 3\alpha_2 + 2\alpha_3$ is satisfied. Now, the dark-soliton solution is identified as the black soliton

$$\psi_0(\zeta,\tau)=B\tanh[B\tau-Q(\zeta)]\exp[i\vartheta(\zeta)], \qquad (28)$$

where

$$Q(\zeta)=\frac{1}{3}\alpha_1 B^3\zeta, \quad \vartheta(\zeta)=B^2\zeta.$$

Here B denotes the amplitude of the background field. As has been known, a dark soliton is a kink-type solution connecting two stable background waves of the same amplitude but of different phases. By considering the phase shift $\phi=\pi$ for the black soliton, Eq. (28) can be rewritten as [13,21]

$$\psi_0(\zeta,\tau)=B\left[\sin\frac{\phi}{2}\tanh\left(B\tau\sin\frac{\phi}{2}-Q\right)+i\cos\frac{\phi}{2}\right]$$
$$\times\exp[i\vartheta(\zeta)]. \qquad (29)$$

Furthermore, the projection functions for the soliton parameters $P_i\in\{B,\vartheta,Q,\phi\}$ can be expressed as

$$f_B=[\tanh(B\tau-Q)+B\tau\,\mathrm{sech}^2(B\tau-Q)]\exp(i\vartheta),$$

$$f_\vartheta=iB\tanh(B\tau-Q)\exp(i\vartheta),$$

$$f_Q=-B\,\mathrm{sech}^2(B\tau-Q)\exp(i\vartheta), \qquad (30)$$

$$f_\phi=-\frac{i}{2}B\exp(i\vartheta).$$

It is interesting that we can construct a set of adjoint functions which can overcome the nonvanishing boundary condition in the forms

$$\overline{f_B}=\frac{9B}{3+\pi^2}(B\tau-Q)\mathrm{sech}^2(B\tau-Q)\exp(i\vartheta),$$

$$\overline{f_\vartheta}=i(B\tau-Q)\mathrm{sech}^2(B\tau-Q)\exp(i\vartheta),$$

$$\overline{f_Q}=\left[-\frac{3}{4}+\frac{9Q}{3+\pi^2}(B\tau-Q)\right]\mathrm{sech}^2(B\tau-Q)\exp(i\vartheta),$$
$$(31)$$

$$\overline{f_\phi}=-i\,\mathrm{sech}^2(B\tau-Q)\exp(i\vartheta).$$

In consequence, it follows from Eqs. (30) and (31) that

$$\mathrm{Re}\int_{-\infty}^{\infty}\overline{f_{P_i}}^*(\zeta,\tau)f_{P_j}(\zeta,\tau)d\tau=\delta_{i,j}. \qquad (32)$$

By using Eqs. (30)–(32) and combining Eq. (15), with the same procedures as for bright solitons, the evolution equations for the soliton parameters ($\alpha_0=-1$) can be given by

$$[\Delta B]_\zeta=\Gamma_B(\zeta),$$

$$[\Delta\vartheta]_\zeta=2B\Delta B+\frac{1}{3}(\alpha_2+\alpha_3)B^3\Delta\phi+\Gamma_\vartheta(\zeta),$$

$$[\Delta Q]_\zeta=\frac{1}{2}B^2\Delta\phi+\alpha_1 B^2\Delta B+\Gamma_Q(\zeta), \qquad (33)$$

$$[\Delta\phi]_\zeta=\Gamma_\phi(\zeta),$$

where the stochastic terms are defined as

$$\Gamma_{P_i}(\zeta)=\mathrm{Re}\int_{-\infty}^{\infty}\overline{f_{P_i}}^*(\zeta,\tau)\bar{\Gamma}d\tau. \qquad (34)$$

In the same way, the correlations of fluctuations in amplitude and phase shift are found to be

$$\langle\Delta B^*(\zeta)\Delta B(\zeta')\rangle=\frac{9(\pi^2-6)B}{4(3+\pi^2)^2\bar{n}}(1+2\alpha^G\zeta), \quad \zeta<\zeta',$$
$$(35)$$

$$\langle\Delta\phi^*(\zeta)\Delta\phi(\zeta')\rangle=\frac{1}{3\bar{n}B}(1+2\alpha^G\zeta)+\frac{2\mathcal{I}(B)}{\bar{n}}\zeta, \quad \zeta<\zeta'.$$
$$(36)$$

From Eqs. (33), (35), and (36), the mean-square timing jitter for a black soliton can be evaluated. Thus, one has

$$\sigma_Q^2=\langle\Delta Q^*(\zeta)\Delta Q(\zeta)\rangle=\sigma_I^2+\sigma_{GH}^2+\sigma_R^2, \qquad (37)$$

where σ_I^2, σ_{GH}^2, and σ_R^2 read

$$\sigma_I^2=\frac{3}{16\bar{n}B}+\left[\frac{1}{12\bar{n}}+\frac{9(\pi^2-6)\alpha_1^2 B^2}{4(3+\pi^2)^2\bar{n}}\right]B^3\zeta^2,$$

$$\sigma_{GH}^2=\frac{3\alpha^G}{8\bar{n}B}\zeta+\left[\frac{1}{18\bar{n}}+\frac{13(\pi^2-6)\alpha_1^2 B^2}{6(3+\pi^2)^2\bar{n}}\right]\alpha^G B^3\zeta^3, \quad (38)$$

$$\sigma_R^2=\frac{\mathcal{I}(B)}{6\bar{n}}B^4\zeta^3.$$

As in the case of bright solitons, all mean-square jitters in Eq. (38) have a quadratic or cubic growth even though the parameter α_1 vanishes. In contrast, the size of these jitters is smaller than that in the bright-soliton case for the same propagation distance [20,21]. Detailed discussions will be provided in Sec. V.

It should be pointed out that Eqs. (20) and (33) are our main results using perturbation theory, based on the HONLS equation, and are somewhat similar to those in Refs. [13] and [15]. By contrast, these results are derived exactly. The expressions in Eqs. (27) and (38) can be used to evaluate the timing jitter analytically. It has been expected that our results would find more extensive applications in the field of high-speed optical communications. To test our theoretical predictions, we wish to simulate the timing jitter directly, based on the underlying equation (1).

IV. NUMERICAL SIMULATION SCHEME

In this section, we would like to develop and implement an unconditionally stable scheme for simulating the general-

ized NLS equation. The scheme can successfully incorporate both multiplicative and additive noises into the symmetrized split-step Fourier method [27,28]. It has been known that there are two forms of stochastic calculus, i.e., an Ito calculus and a Stratanovich [29,30] calculus. In our simulations, the Stratanovich prescription to integrate the stochastic noise terms is used since its variable changes simply follow the rules of usual calculus. In the following, we outline the basic steps of our algorithm.

The generalized NLS equation including both the multiplicative and additive noise terms can be written in its operator forms

$$\frac{\partial \psi}{\partial \zeta} = (\hat{D} + \hat{N})\psi + \hat{S}_M \psi + \hat{S}_A,$$

$$\hat{D} = \alpha_0 \frac{i}{2} \frac{\partial^2}{\partial \tau^2} + \frac{1}{6} \alpha_1 \frac{\partial^3}{\partial \tau^3} - \gamma,$$

$$\hat{N} = i|\psi|^2 - \frac{\alpha_2}{\psi} \frac{\partial}{\partial \tau}(|\psi|^2 \psi) - \alpha_3 \frac{\partial}{\partial \tau}(|\psi|^2), \qquad (39)$$

$$\hat{S}_M = i\Gamma^R(\zeta, \tau),$$

$$\hat{S}_A = \Gamma(\zeta, \tau),$$

where $\hat{D}$, $\hat{N}$, $\hat{S}_M$, and $\hat{S}_A$ correspond to the linear (dispersive), nonlinear, multiplicative stochastic, and additive stochastic operators, respectively. It has an exact solution for infinitesimal $\Delta \zeta$ given by

$$\psi(\zeta + \Delta \zeta, \tau) = \exp[\Delta \zeta(\hat{D} + \hat{N})]\psi(\zeta, \tau)$$

$$+ \int_\zeta^{\zeta + \Delta \zeta} [\hat{S}_M \psi(\zeta, \tau) + \hat{S}_A]d\zeta. \qquad (40)$$

To carry out our simulations, solution (40) is further approximated in a symmetrical form

$$\psi(\zeta + \Delta \zeta, \tau) \simeq \exp\left[\frac{1}{2}\Delta \zeta \hat{D}\right]\exp[\Delta \zeta \hat{N}_m]\exp\left[\frac{1}{2}\Delta \zeta \hat{D}\right]\psi(\zeta, \tau)$$

$$+ \Delta W_M \bar{\psi}_m + \Delta W_A, \qquad (41)$$

where

$$\Delta W_M = \frac{1}{\Delta \tau} \int_\tau^{\tau + \Delta \tau} \int_\zeta^{\zeta + \Delta \zeta} \hat{S}_M(\zeta, \tau)d\tau d\zeta,$$

$$\Delta W_A = \frac{1}{\Delta \tau} \int_\tau^{\tau + \Delta \tau} \int_\zeta^{\zeta + \Delta \zeta} \hat{S}_A(\zeta, \tau)d\tau d\zeta,$$

$$\hat{N}_m = \frac{1}{2}[\hat{N}(\zeta, \tau) + \hat{N}(\zeta + \Delta \zeta, \tau)], \qquad (42)$$

$$\bar{\psi}_m = \frac{1}{2}[\psi(\zeta, \tau) + \psi(\zeta + \Delta \zeta, \tau)].$$

It has been noted that our symmetrized form of Eq. (41) has two advantages at least. One is that the leading error is of third order in the step size $\Delta \zeta$. The other is that the implementation is unconditionally stable since a semi-implicit method is used in $\hat{N}_m$ and $\bar{\psi}_m$ [27,29]. Furthermore, the integrals for the multiplicative and additive noises in Eq. (42) are discretized in a one-dimensional lattice of $N = 2^p$ (p is a positive integer) cells, where the lattice spacing is $\Delta \tau = T/N$ with T being the lattice length. The resulting versions take the forms

$$\Delta W_{M,jm} = \frac{1}{\Delta \tau} \int_{\tau_j}^{\tau_j + \Delta \tau} \int_{\zeta_m}^{\zeta_m + \Delta \zeta} \hat{S}_M(\zeta, \tau)d\tau d\zeta,$$

$$\Delta W_{A,jm} = \frac{1}{\Delta \tau} \int_{\tau_j}^{\tau_j + \Delta \tau} \int_{\zeta_m}^{\zeta_m + \Delta \zeta} \hat{S}_A(\zeta, \tau)d\tau d\zeta. \qquad (43)$$

By means of Eq. (2), the correlations of these noise terms can be expressed as

$$\langle W_{M,jm}^* W_{M,j'm'} \rangle = \frac{2\varepsilon \delta_{jj'} \delta_{mm'} \Delta \zeta}{\bar{n} \Delta \tau},$$

$$\langle W_{A,jm}^* W_{A,j'm'} \rangle = \frac{\alpha^G \delta_{jj'} \delta_{mm'} \Delta \zeta}{\bar{n} \Delta \tau}. \qquad (44)$$

It has been assumed that the noises are Gaussian white with respect to time and space, meanwhile the time correlation function is taken as $F(\tau - \tau') = 2\varepsilon \delta(\tau - \tau')$, where $\varepsilon = 4.6 \times 10^{-2}$ at a temperature of 300 K [13]. Techniques for the efficient generation of Gaussian white noise have been heavily investigated since the 1960s [29,30]. In this paper, we obtain noises directly with various intensities from the computer-based Gaussian random generator, e.g., the NORMRND function in MATLAB software. In fact, the spatiotemporal colored noise can also be generated efficiently in this way, according to a robust algorithm developed by García-Ojalvo *et al.* [31].

On the other hand, the execution of the exponential operator $\exp[\Delta \zeta \hat{D}/2]$ is carried out in Fourier space by using the prescription

$$\exp\left[\frac{1}{2}\Delta \zeta \hat{D}\right]B(\zeta, \tau) = \left\{\mathcal{F}^{-1} \exp\left[\frac{1}{2}\Delta \zeta \hat{D}(i\omega)\right]\mathcal{F}\right\}B(\zeta, \tau), \qquad (45)$$

where $\mathcal{F}$ denotes the Fourier-transform operation, and $\hat{D}(i\omega)$ is obtained by replacing $(\partial/\partial \tau)$ by $i\omega$. Considering its discrete version, we employ the fast Fourier transform (FFT) algorithm [32] to implement Eq. (45) efficiently, where a high-frequency cutoff is used in an equivalent ω lattice. Because of the nonvanishing boundary condition at $\tau = \pm T/2$, the discrete values ω_k for dark solitons with k running from 1 to N in the FFT algorithm are different from those for bright cousins. More specifically, ω_k should be odd multiples of π/T for dark solitons and even multiples for bright solitons, but with the same spacing $\Delta \omega = 2\pi/T$ along the ω

lattice. In the mean time, great care is taken to treat the FFT approximation to the Fourier form of Eq. (45) for different solitons [29]. The other executions of the stochastic and non-linear operators, i.e., $\hat{S}_M$, $\hat{S}_A$, and $\hat{N}$, are carried out in τ space, and an iterated root-finding mechanism is adopted to evaluate the semi-implicit steps in $\hat{N}_m$ and $\bar{\psi}_m$ [27,29].

As can be seen, it is rather straightforward, though a little time-consuming, to simulate the stabilities for bright and dark solitons. Therein we have chosen 0.04 and 0.005 as discretization time and space meshes, respectively, to reduce the discretization error. By considering the initial fluctuations in soliton parameters derived from Eq. (22), the initial wave functions for bright and dark solitons can be written as

$$\psi^{\mathrm{bri}}(0,\tau)=(1+\delta A)\mathrm{sech}[(1+\delta A)\tau+\delta q]\exp(-i\,\delta\Omega\,\tau),$$

(46)

$$\psi^{\mathrm{dar}}(0,\tau)=(1+\delta B)\tanh[(1+\delta B)\tau-\delta Q]\exp(-i\,\delta\varpi\,\tau),$$

(47)

where $\delta A=(1/\sqrt{2\bar{n}})\delta\rho_1$, $\delta q=(\pi/\sqrt{24\bar{n}})\delta\rho_2$, $\delta\Omega=(1/\sqrt{6\bar{n}})\delta\rho_3$, $\delta B=[9(\pi^2-6)/4(3+\pi^2)^2\bar{n}]^{1/2}\delta\rho_4$, $\delta Q=\sqrt{3/16\bar{n}}\delta\rho_5$, and $\delta\varpi=(1/\sqrt{12\bar{n}})\delta\rho_6$. Here $\delta\rho_i$ $(i=1,\ldots,6)$ are Gaussian-independent random numbers of zero mean and variance equal to one. The simulating results of stabilities under these initial conditions have been shown in Figs. 1, 2 and 3 (see Sec. II).

For numerical evaluation of timing jitter, besides the same two steps and initial conditions as exploited above, we have used the ensemble which is of 500 trajectories to reduce sampling error, within a small distance of propagation ($\simeq$10 km). These values result from a compromise between time calculation and accuracy. Besides, care should be taken to simulate the timing jitter for either type of solitons since each has a different expression for jitter variance. In the concrete, the variance of timing jitter is generally defined as $\sigma_t^2=\langle t_p^2\rangle-\langle t_p\rangle^2$, where the symbol $\langle\ \rangle$ denotes the so-called ensemble average and t_p is the pulse position. For bright solitons, $t_p=(1/E)\int_{-\infty}^{\infty}\tau|\psi|^2\,d\tau$, where $E=\int_{-\infty}^{\infty}|\psi|^2\,d\tau$ denotes the pulse energy [19]. It is noted that for dark solitons this center-of-mass method can only give information on the global energy distribution but not on the dark-pulse position itself [20]. Fortunately, in our simulations we can modify the formula t_p for bright solitons so that it is valid for dark solitons. We have $t_p=(1/E)\int_{-\infty}^{\infty}\tau\,\mathrm{sech}^2(\tau-Q)|\psi|^2\,d\tau$, where $E=\int_{-\infty}^{\infty}\mathrm{sech}^2(\tau-Q)|\psi|^2\,d\tau$. The multiplier $\mathrm{sech}^2(\tau-Q)$, $(Q=\alpha_1\zeta/3)$, is adopted to eliminate the effects of the highly undulating cw background and overcome the nonvanishing boundary condition (see Fig. 2). For longer distances ($>$100 dispersion lengths), alternatively we can employ the strategies taken by Hamaide *et al.* [20], where the pulse position is roughly found by means of a certain threshold condition. The numerical illustrations of timing jitter in terms of these expressions will be shown in Sec. V.

V. DISCUSSIONS

It is well-known that apart from optical losses or dissipation, timing jitter is the key factor which limits the total transmission distance of the soliton link. From Eqs. (26) and (37), we can see that there are three physical mechanisms which induce deviations in the soliton position from its original location at the bit center. One is the vacuum fluctuations, resulting from the Heisenberg uncertainty principle and being important for small propagation distances. The second is the Gordon-Haus noise which comes from the gain and loss in the fiber and produces the well known Gordon-Haus jitter [14]. In the long-distance soliton communications it is essential for relatively long ($>$10 ps) pulses. The last is the Raman noise which originates from the intrinsic thermal quantum fluctuations of phonon reservoirs and generates the cubic growth in jitter variance, just like the Gordon-Haus noise. The magnitude of the Raman jitter can be obtained by evaluating the overlap integral $\mathcal{I}(X)$ analytically or numerically. For simplicity, we use a single-Lorentzian model in our analytical work and find $\mathcal{I}(X)=(4/15)X\varepsilon$, where $X=A$ or B [13].

Owing to the influences of these higher-order effects, the expressions of timing jitters are all a little different from those obtained by using the perturbation theory of the NLS equation [13,15]. For comparison, we summarize these noise sources which have different characteristic scaling properties in the following.

A. Vacuum fluctuations

For bright solitons the mean-square timing jitter resulting from the vacuum fluctuations is given by

$$\sigma_{I(\mathrm{bri})}^2=\frac{\pi^2}{24\bar{n}}+\left[\frac{1}{6\bar{n}}+\frac{\alpha_1^2}{8\bar{n}}\right]\zeta^2.$$

(48)

Correspondingly, the mean-square fluctuations for dark solitons read

$$\sigma_{I(\mathrm{dar})}^2=\frac{3}{16\bar{n}}+\left[\frac{1}{12\bar{n}}+\frac{9(\pi^2-6)\alpha_1^2}{4(3+\pi^2)^2\bar{n}}\right]\zeta^2.$$

(49)

It is clear that the mean-square fluctuations depend not only on the quadratic growth in distance ζ, but also on α_1^2 for both bright and dark solitons. As seen, the vacuum fluctuations originate from three fundamental contributions. One is the initial position fluctuations, while the other two come from initial fluctuations in soliton frequency (or phase difference ϕ) and amplitude, respectively. As one might expect, amplitude fluctuations also lead to a degradation of the signal-to-noise of the soliton bit stream [17–19]. After a simple calculation, we can see that the vacuum jitter variance for dark solitons is nearly one half of that for bright solitons at the same propagation distance.

B. Gordon-Haus noise

When the reservoir gain and loss are considered, there appears the well-known Gordon-Haus jitter in the fiber since

the optical amplifiers add both the amplitude and phase noises to the amplified soliton. Currently, this jitter is the major limiting factor that affects the performance of soliton communications and the total transmission distance. From Eqs. (27) and (38), we can immediately obtain the Gordon-Haus jitter variance for bright and dark solitons:

$$\sigma^2_{GH(\text{bri})} = \frac{\pi^2 \alpha^G}{12\bar{n}} \zeta + \left[\frac{1}{9\bar{n}} + \frac{13\alpha_1^2}{108\bar{n}} \right] \alpha^G \zeta^3, \qquad (50)$$

$$\sigma^2_{GH(\text{dar})} = \frac{3\alpha^G}{8\bar{n}} \zeta + \left[\frac{1}{18\bar{n}} + \frac{13(\pi^2-6)\alpha_1^2}{6(3+\pi^2)^2\bar{n}} \right] \alpha^G \zeta^3. \quad (51)$$

In the presence of higher-order effects, the mean-square Gordon-Haus jitters for both bright and dark solitons have an extra cubic growth, which depends on α_1^2 and becomes important over a long distance. Like the case of vacuum fluctuations, the ratio between Eq. (51) and Eq. (50) ranges from 0.42 to 0.5.

C. Raman noise

A lesser-known fluctuation effect that arises from the Raman phase-noise term Γ^R induces the Raman jitter in optical communications. The Raman jitter is different from the Gordon-Haus jitter and independent of all higher-order effects in our current system. Substituting $\mathcal{I}(X) = (4/15)X\varepsilon$ into the third formulas in Eqs. (27) and (38) and letting A and $B = 1$ yields

$$\sigma^2_{R(\text{bri})} = \frac{8}{45\bar{n}} \varepsilon \zeta^3, \qquad (52)$$

$$\sigma^2_{R(\text{dar})} = \frac{2}{45\bar{n}} \varepsilon \zeta^3. \qquad (53)$$

Compared to Gordon-Haus case, the mean-square Raman jitter for dark solitons is only 1/4 of that for bright solitons. Moreover, it is easy to follow from Eqs. (50) and (52) [or Eqs. (51) and (53)] that the Raman jitter dominates the Gordon-Haus jitter in the femtosecond regime. However, when the soliton duration is of picosecond order, the case is the opposite. The physical reason for these effects is simple. Solitons have an intensity that increases with the dispersion if everything else is unchanged. Meanwhile, the multiplicative phase noise found in Raman propagation is proportional to the intensity and hence becomes relatively large as compared to the Gordon-Haus jitter that depends on the additive stochastic term. Therefore, for large enough dispersion, corresponding to the high intensity, the Raman jitter should become readily observable at short enough distances while the Gordon-Haus jitter is relatively small.

For $T_0 = 500$ fs bright and dark solitons, typically, the TOD parameter is $\alpha_1 = \mp 9.6 \times 10^{-3}$, and the other parameters are given by $\alpha_2 = 3.18 \times 10^{-3}$, $\alpha_3 = (\mp\alpha_1 - 3\alpha_2)/2$, $\alpha^G/L_D = 4.6 \times 10^{-5}$ (i.e., 0.2 dB/km at commonly used wavelength $\lambda = 1.55$ μm), and $\bar{n} = 3 \times 10^6$, with $L_D = 500$ m. These parameters are evaluated based on $|\beta_2| = 0.5$ ps^2/km, $\beta_3 = \mp 0.0024$ ps^3/km (negative for bright
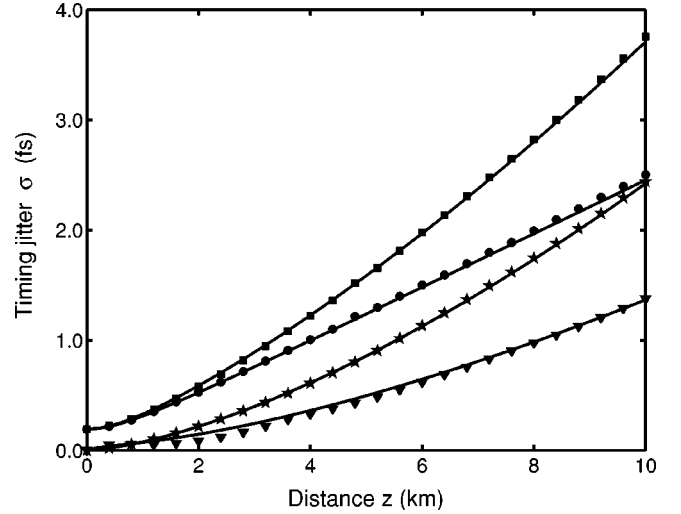

FIG. 5. Timing jitter for the 500-fs bright soliton as a function of the transmission distance. The total jitter (squares), vacuum fluctuations (circles), Raman jitter (stars) and Gordon-Haus jitter (triangles) come from our numerical simulations based on Eq. (1), where $\Delta\zeta = 0.04$ and $\Delta\tau = 0.005$. The statistical ensemble is of 500 trajectories and other parameters are specified in the text. For comparison, our analytical results (solid lines) are plotted.

and positive for dark solitons), $A_{\text{eff}} = 40$ μm^2, and $n_2 = 2.6 \times 10^{-20}$ m^2/W for a dispersion-shifted fiber. By utilizing these parameters, all jitters including the vacuum fluctuations, Gordon-Haus jitter and Raman jitter for $T_0 = 500$ fs bright and dark solitons are depicted both numerically and analytically, as shown in Figs. 5 and 6, respectively. Also, the total jitter corresponding to the realistic case in which all three noise sources are active is demonstrated there. In Figs.
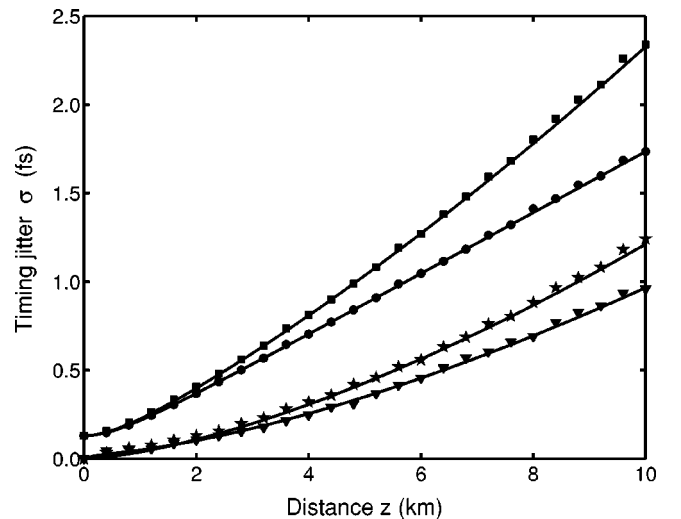

FIG. 6. Timing jitter for the 500-fs dark soliton as a function of transmission distance. The total jitter (squares), vacuum fluctuations (circles), Raman jitter (stars), and Gordon-Haus jitter (triangles) correspond to our numerical simulations, where the discretized steps and ensemble are the same as in Fig. 5. The other parameters are specified in the text. For comparison, our analytical results (solid lines) are plotted here.

5 and 6, it is clear to see that the Gordon-Haus jitter in dark solitons is nearly $1/\sqrt{2}$ of the corresponding one in bright solitons [20,21]. Meantime, the Raman jitter for femtosecond solitons exceeds the corresponding Gordon-Haus one. Moreover, all numerical simulations are in excellent agreement with analytical solutions derived from the extended perturbation model. For extremely ultrafast pulses (<100 fs), these higher-order effects become of considerable importance; therefore the complex property of coefficients α_2 and α_3 in Eq. (1) should be taken into account [16]. To do this with this model is still an open problem and is under investigation.

From Eqs. (20) and (33), it is of interest to note that the timing jitter in femtosecond soliton communications can be reduced considerably when the frequency fluctuations (or phase fluctuations) are confined to a vanishingly small range by using some effective techniques for soliton control such as filtering and optical phase conjugation [18]. As a result, the timing jitter originates mostly from amplitude fluctuations imposed on solitons, because now the dominant contributions come mainly from the terms proportional to α_1^2. This theoretical prediction is well consistent with the conclusion drawn by Agrawal *et al.* [18].

VI. CONCLUSIONS

In this paper, we have developed an extended soliton perturbation model based on the HONLS equation. The evolution equations for the soliton parameters and the resultant expressions for timing jitter have been derived for the first time, to our knowledge. Subsequently, the model has been tested to be correct in subpicosecond-femtosecond regime through direct numerical simulations of the underlying equation by using the stochastic split-step Fourier method. It is shown that the results of our numerical simulations are in excellent agreement with analytical predictions for timing jitter. We found that the Gordon-Haus jitter for dark solitons is nearly $1/\sqrt{2}$ of that for bright solitons and the Raman jitter always dominates the Gordon-Haus jitter in femtosecond regime. In particular, the stabilities of the solitary waves have been demonstrated under the Gaussian white noise. In the picosecond regime, our theoretical predictions coincide with those obtained in Refs. [13] and [15]. It is expected that for bright and dark solitons, the present equations of motion would find extensive applications in the high-speed communication systems more than those obtained by use of the perturbation theory about the NLS equation.

APPENDIX

In this appendix, we would like to outline the proof of Eq. (20). In order to prove the first formula, we integrate both sides of Eq. (15) with the operation $\int_{-\infty}^{\infty} d\tau \overline{f_A}^*(\tau,\zeta)$, utilizing the parities of the integral kernels. By taking the real part of the integral equation and using the orthogonal relation Eq.

(19), with some tedious manipulations, the resulting terms related to Eq. (15) can be written as

$$\mathrm{Re}\int_{-\infty}^{\infty}\overline{f_A}^*[\Delta\psi]_\zeta\,d\tau=[\Delta A]_\zeta+\mathrm{Re}\int_{-\infty}^{\infty}\overline{f_A}^*[f_A]_\zeta\Delta A\,d\tau$$

$$+\mathrm{Re}\int_{-\infty}^{\infty}\overline{f_A}^*[f_\theta]_\zeta\Delta\theta\,d\tau$$

$$+\mathrm{Re}\int_{-\infty}^{\infty}\overline{f_A}^*[f_q]_\zeta\Delta q\,d\tau$$

$$+\mathrm{Re}\int_{-\infty}^{\infty}\overline{f_A}^*[f_\Omega]_\zeta\Delta\Omega\,d\tau$$

$$=[\Delta A]_\zeta+\frac{1}{9}\alpha_1 A^3 q\Delta A-A^3\Delta\theta$$

$$-\frac{1}{9}\alpha_1 A^4\Delta q-A^2 q\Delta\Omega, \qquad \text{(A1)}$$

$$\mathrm{Re}\int_{-\infty}^{\infty}\frac{i}{2}\overline{f_A}^*[\Delta\psi]_{\tau\tau}\,d\tau=\frac{1}{3}A^3\Delta\theta+\frac{1}{3}A^2 q\Delta\Omega, \quad \text{(A2)}$$

$$\mathrm{Re}\int_{-\infty}^{\infty}i\overline{f_A}^*[\psi_0^2\Delta\psi^*+2|\psi_0|^2\Delta\psi]d\tau$$

$$=-\frac{4}{3}A^3\Delta\theta-\frac{4}{3}A^2 q\Delta\Omega, \qquad \text{(A3)}$$

$$\mathrm{Re}\int_{-\infty}^{\infty}\frac{\alpha_1}{6}\overline{f_A}^*[\Delta\psi]_{\tau\tau\tau}\,d\tau=-\frac{7}{45}\alpha_1 A^3 q\Delta A+\frac{7}{45}\alpha_1 A^4\Delta q,$$

$$\text{(A4)}$$

$$\mathrm{Re}\int_{-\infty}^{\infty}\alpha_2\overline{f_A}^*[\psi_0^2\Delta\psi^*+2|\psi_0|^2\Delta\psi]_\tau\,d\tau$$

$$=\frac{4}{5}\alpha_2 A^3 q\Delta A-\frac{4}{5}\alpha_2 A^4\Delta q, \qquad \text{(A5)}$$

$$\mathrm{Re}\int_{-\infty}^{\infty}\alpha_3\overline{f_A}^*[|\psi_0|^2]_\tau\Delta\psi\,d\tau$$

$$=-\frac{8}{15}\alpha_3 A^3 q\Delta A+\frac{8}{15}\alpha_3 A^4\Delta q, \qquad \text{(A6)}$$

$$\mathrm{Re}\int_{-\infty}^{\infty}\alpha_3\overline{f_A}^*[\psi_0^*\Delta\psi+\psi_0\Delta\psi^*]_\tau\psi_0\,d\tau$$

$$=\frac{16}{15}\alpha_3 A^3 q\Delta A-\frac{16}{15}\alpha_3 A^4\Delta q, \qquad \text{(A7)}$$

where all quantities ΔA, $\Delta\theta$, Δq and $\Delta\Omega$ are real functions of distance ζ. By substituting Eqs. (A1)–(A7) into the integral equation and using the relation $\alpha_1=-(3\alpha_2+2\alpha_3)$, the first formula, $[\Delta A(\zeta)]_\zeta=\Gamma_A$, can be obtained readily. Similarly, the other three formulas in Eq. (20) can be proved.

[1] A.I. Maimistov and M. Basharov, *Nonlinear Optical Waves* (Kluwer, Dordrecht, 1999).

[2] A. Hasegawa and F.D. Tappert, Appl. Phys. Lett. **23**, 142 (1973).

[3] S.L. McCall and E.L. Hahn, Phys. Rev. Lett. **18**, 908 (1967).

[4] D. Anderson and M. Lisak, Phys. Rev. A **27**, 1393 (1983), and references therein.

[5] F.M. Mitschke and L.F. Mollenauer, Opt. Lett. **11**, 659 (1986); J.P. Gordon, *ibid.* **11**, 662 (1986).

[6] Y. Kodama and A. Hasegawa, IEEE J. Quantum Electron. **23**, 510 (1987).

[7] D. Mihalache, N. Truta, and L.-C. Crasovan, Phys. Rev. E **56**, 1064 (1997).

[8] M. Gedalin, T.C. Scott, and Y.B. Band, Phys. Rev. Lett. **78**, 448 (1997).

[9] S.L. Palacios, A. Guinea, J.M. Fernández-Díaz, and R.D. Crespo, Phys. Rev. E **60**, R45 (1999).

[10] K. Porsezian and K. Nakkeeran, Phys. Rev. Lett. **76**, 3955 (1996); **74**, 2941 (1995).

[11] Z.H. Li, L. Li, H.P. Tian, and G.S. Zhou, Phys. Rev. Lett. **84**, 4096 (2000).

[12] H.A. Haus and Y. Lai, J. Opt. Soc. Am. B **7**, 386 (1990).

[13] J.E. Corney and P.D. Drummond, J. Opt. Soc. Am. B **18**, 153 (2001); P.D. Drummond and J.E. Corney, *ibid.* **18**, 139 (2001).

[14] J.P. Gordon and H.A. Haus, Opt. Lett. **11**, 665 (1986); A. Mecozzi, J.D. Moores, H.A. Haus, and Y. Lai, *ibid.* **16**, 1841 (1991).

[15] H.A. Haus and W.S. Wong, Rev. Mod. Phys. **68**, 423 (1996).

[16] Z.H. Li, L. Li, H.P. Tian, G.S. Zhou, and K.H. Spatschek, Phys. Rev. Lett. **89**, 263901 (2002).

[17] D. Mihalache, L.-C. Crasovan, N.-C. Panoiu, F. Moldoveanu, and D.-M. Baboiu, Opt. Eng. **35**, 1611 (1996).

[18] See, for example, *Progress in Optics*, edited by E. Wolf (North-Holland, Amsterdam, 1997), Vol. XXXVII, p. 185; R.-J. Essiambre and G.P. Agrawal, J. Opt. Soc. Am. B **14**, 314 (1997); **14**, 323 (1997).

[19] V.S. Grigoryan, C.R. Menyuk, and R.M. Mu, J. Lightwave Technol. **17**, 1347 (1999); J. Santhanam and G.P. Agrawal, J. Opt. Soc. Am. B **20**, 284 (2003), and references therein.

[20] J.P. Hamaide, P. Emplit, and M. Haelterman, Opt. Lett. **16**, 1578 (1991).

[21] Y.S. Kivshar, M. Haelterman, P. Emplit, and J.P. Hamaide, Opt. Lett. **19**, 19 (1994).

[22] L. Mandel and E. Wolf, *Optical Coherence and Quantum Optics* (Cambridge University Press, Cambridge, England, 1995), Chap. 3.

[23] R.H. Stolen and M.A. Bösch, Phys. Rev. Lett. **48**, 805 (1982); R.H. Stolen, J.P. Gordon, W.J. Tomlinson, and H.A. Haus, J. Opt. Soc. Am. B **6**, 1159 (1989).

[24] H.R. Brand and R.J. Deissler, Phys. Rev. Lett. **63**, 2801 (1989).

[25] Y.S. Kivshar, D.E. Pelinovsky, T. Cretegny, and M. Peyrard, Phys. Rev. Lett. **80**, 5032 (1998).

[26] D.J. Kaup, Phys. Rev. A **42**, 5689 (1990); D. Mihalache, N.-C. Panoiu, F. Moldoveanu, and D.-M. Baboiu, J. Phys. A **27**, 6177 (1994).

[27] G.P. Agrawal, *Nonlinear Fiber Optics* (Academic, San Diego, 1989).

[28] B. Khubchandani, P.N. Guzdar, and R. Roy, Phys. Rev. E **66**, 066609 (2002).

[29] P.D. Drummond and I.K. Mortimer, J. Comput. Phys. **93**, 144 (1991); M.J. Werner and P.D. Drummond, *ibid.* **132**, 312 (1997).

[30] K. Ito, *Lectures on Stochastic Processes* (Tata Institute of Fundamental Research, Bombay, 1960); R.L. Stratanovich, *Topics in the Theory of Random Noise* (Gordon & Breach, New York, 1963), Vols. I and II.

[31] J. García Ojalvo, J.M. Sancho, and L. Ramírez-Piscina, Phys. Rev. A **46**, 4670 (1992).

[32] J.W. Cooley and J.W. Tukey, Math. Comput. **19**, 297 (1965); J.W. Cooley, P.A.W. Lewis, and P.D. Welch, IEEE Trans. Educ. **12**, 27 (1969).